J Mater Sci: Mater Med (2007) 18:1771–1779
DOI 10.1007/s10856-007-3040-7

Influence of polyelectrolyte on the thermosensitive property of PNIPAAm-based copolymer hydrogels

Xian-Zheng Zhang · Chih-Chang Chu

Received: 23 January 2006 / Accepted: 5 May 2006 / Published online: 5 May 2007

Abstract A new family of poly(NIPAAm-co-2-acrylamido-2-methyl-1-propanesulfonic acid) [P(NIPAAm-co-AMPSA)] hydrogels was synthesized by incorporating negative charged AMPSA to the backbone of the PNIPAAm-based hydrogel. The effect of polyelectrolyte (i.e., PAMPSA) on the thermosensitive property of PNIPAAm hydrogels was investigated. It was found that P(NIPAAm-co-AMPSA) hydrogels exhibited unique honey-comb-like 3D porous structure having rigid cell wall as well as enhanced mechanical property. The incorporation of AMPSA into PNIPAAm backbones also led to a significant increase in swelling capability at room temperature when comparing to pure PNIPAAm hydrogels. In addition, the shrinking rate upon heating was significantly improved if the AMPSA content in P(NIPAAm-co-AMPSA) hydrogels was less than 10 wt%.

Introduction

Hydrogels are hydrophilic, polymeric networks, capable of imbibing large amounts of water or biological fluids [1–4]. A stimuli-sensitive hydrogel is able to respond to specific external stimuli, such as temperature, pH, electric field, and antigen [5–9]. The stimuli-sensitive hydrogels exhibit dramatic changes in their swelling behavior, network structure, permeability and/or mechanical property over a range of stimulus values; polymers having this unique intelligent property have received extensive interest during the last decade.

Temperature sensitive hydrogels are the most extensively studied stimuli-sensitive materials. Poly(N-isopropylacrylamide) (PNIPAAm) hydrogel is temperature sensitive, which exhibits a lower critical solution temperature (LCST) at around 33 °C [10]. In PNIPAAm polymer chains, there exists an optimum hydrophilic/hydrophobic balance between hydrophilic groups (amide, -CONH-) and hydrophobic groups (isopropyl, $-CH(CH_3)_2$) [11]. Below LCST, hydrogen bonding between water molecules and hydrophilic segments (amide-, -CONH-) of the PNIPAAm polymer chains becomes dominant, which leads to dissolution of PNIPAAm in water [12, 13]. At LCST, hydrogen bonding between the polymer and water becomes unfavorable compared to polymer-polymer interaction and water-water interactions. Above LCST, the hydrophobic groups in the polymer chains (isopropyl groups) aggregate and become insoluble in water [12, 13]. This unique temperature-induced phase separation of PNIPAAm also appears in PNIPAAm-based hydrogels and has been used in various biomedical fields, including protein-ligand recognition, drug controlled release, recovered and cultured cells and immobilization enzymes [14–19].

PNIPAAm is a class of non-ionic polymers, while polyelectrolytes are a class of ionic polymers having positive or negative charges, which give rise to property distinct from those of non-ionic polymers [20]. By binding with oppositely charged materials, polyelectrolytes have widely applications in biomedical technology, such as cell adhesive and non-adhesive polymers [21, 22]. A strategy to

X.-Z. Zhang
Key Laboratory of Biomedical Polymers of Ministry of Education & Department of Chemistry, Wuhan University, Wuhan 430072, P.R. China

X.-Z. Zhang · C.-C. Chu (✉)
Department of Textiles and Apparel & Biomedical Engineering Program, Cornell University, Ithaca, NY 14853-4401, USA
e-mail: cc62@cornell.edu

modify cell adhesion to substrates is to impart an electric charge to a network scaffold [23]. In addition, when an external electric field is applied, the charged hydrogel system has been utilized to fabricate chemomechanical devices with various kinds of motion [24–26]. For example, such a hydrogel may be used as an artificial muscle since it is able to convert chemical energy to mechanical energy; in other words, under a directed electric field, such hydrogel systems can move with a worm-like motion [24].

Consequently, it is of particular interest to examine the influence of incorporated polyelectrolyte segment on the thermo-sensitive property of PNIPAAm hydrogels. In this paper, we reported the synthesis of a new family of poly(NIPAAm-co-2-acrylamido-2-methyl-1-propanesulfonic acid) [P(NIPAAm-co-AMPSA)] hydrogel by incorporating the negatively-charged AMPSA segment into the backbone of PNIPAAm hydrogel. The effect of the feed ratio of NIPAAm to AMPSA monomers on the property of the resultant P(NIPAAm-co-AMPSA) hydrogels was examined in terms of LCST via differential scanning calorimetry (DSC), morphology via scanning electron microscopy (SEM), mechanical property via compression modulus measurement, and swelling profiles and kinetics.

Materials and methods

Materials

N-isopropylacrylamide purchased (NIPAAm, Aldrich Chemical, USA) was further purified by recrystallization in benzene/n-hexane. 2-Acrylamido-2-methyl-1-propanesulfonic acid (AMPSA), *N*, *N*′-methylenebisacrylamide (MBAAm), ammonium persulfate (APS) and *N*, *N*, *N*′, *N*′-tetramethylethylenediamine (TEMED) were purchased from Sigma Chemical Company (St. Louis, Missouri, USA). All the reagents used were of analytical grade, unless otherwise stated.

Hydrogel fabrications

P(NIPAAm-co-AMPSA) hydrogels were prepared in a phosphate buffer solution of NIPAAm and AMPSA precursors in the presence of MBAAm crosslinker at room temperature (22 °C). In brief, precursors NIPAAm and AMPSA, crosslinker MBAAm and initiator APS were dissolved in a phosphate buffer solution (PBS, pH 7.4 and ionic strength $I = 0.1$) to make a clear precursor solution. TEMED was subsequently added into the precursor solution and the reaction glass bottle was sealed for carrying out the copolymerization/crosslinking reaction for 12 h at room temperature (Scheme 1). After the reaction, the solid hydrogels synthesized were washed with PBS solution at room temperature and PBS solution was replaced with fresh one every several hours to remove any unreacted chemicals within the hydrogel matrix. The washed hydrogels were cut into disc-shape of approximately 12 mm in diameter and 4 mm in thickness for the following characterization study. The resultant P(NIPAAm-co-AMPSA) hydrogels were labeled as Gel_x, where x indicated the AMPSA content (wt% based on precursors amount of NIPAAm and AMPSA). The precursor feed composition and preparation conditions of P(NIPAAm-co-AMPSA) hydrogels were summarized in Table 1. Pure PNIPAAm hydrogel was prepared in the same manner, except in the absence of AMPSA and was labeled as Gel_0 and used as control.

Table 1 Feed compositions and sample ID of P(NIPAAm-co-AMPSA) hydrogels

	Sample ID[a]				
	Gel_0	$Gel_{2.5}$	Gel_5	Gel_{10}	Gel_{15}
NIPAAm (mg)	200	195	190	180	170
AMPSA (mg)	0	5	10	20	30
MBAAm (mg)	5.0	5.0	5.0	5.0	5.0
PBS7.4 (ml)	2.0	2.0	2.0	2.0	2.0
10.0 wt% APS solution (μl)	10	10	10	10	10
TEMED (μl)	5	5	5	5	5
Conversion (%)[b]	88.3	87.8	88.3	91.8	90.7

[a] All reactions were carried out for 12 h at room temperature (22 °C)

[b] Weight percentage of the synthesized hydrogel from the monomers

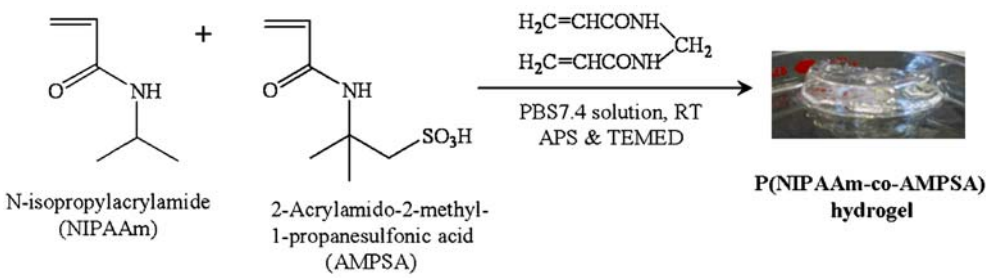

Scheme 1 Chemical structures and schematic preparation of P(NIPAAm-co-AMPSA) hydrogels

LCST determination

Differential scanning calorimeter (DSC, TA model 2920) was used to determine the LCST of P(NIPAAm-co-AMPSA) hydrogels. A known weight of an equilibrated swollen hydrogel sample (~10 mg) in PBS solution was placed in a hermetic aluminum pan and sealed by a hermetic aluminum lid. The sample was heated from 15 to 65 °C at a rate of 3 °C/min in a nitrogen environment. The temperature-induced collapse of the hydrogel at its LCST was recorded by the appearance of an endotherm peak in a DSC thermogram. TA universal analysis software was used for the data acquisition and analysis.

SEM observation of interior morphologies

The P(NIPAAm-co-AMPSA) hydrogel samples prepared above were first equilibrated in PBS solution (pH 7.4) at room temperature to reach an equilibrium state. The equilibrated hydrogel samples were quickly frozen in liquid nitrogen and further freeze-dried under vacuum at –45 °C for 4 days until the solvent was sublimed. The freeze-dried samples were then fractured carefully and their interior morphology was studied by using a scanning electron microscope (Hitachi S4500 SEM, Mountain View, CA). Before SEM observation, hydrogel specimens were fixed on aluminum stubs and coated with gold for 30s under vacuum.

Mechanical property measurement

The mechanical property of the swollen P(NIPAAm-co-AMPSA) hydrogel samples were measured by an Instron tester model 1122 (Instron Corporation, Canton, Massachusetts, USA) at 22 °C and 65% humidity. Before mechanical property experiment, all samples were immersed in PBS solution at room temperature for 3 days to reach their equilibrium state. The uncompressed thickness of the hydrogel was evaluated using a compressometer (Frazier Instruments, Hagerstown, MD). The swollen hydrogel samples were then placed onto the top surface of a compression load cell (5 kg full load capacity) and compressed between this cell and a cylindrical metal parallel probe (diameter = 6.0 mm) at a crosshead speed of 1.0 mm/min until failure or full load was reached. The load and displacement were recorded. The compressive moduli were calculated from the slope of the initial linear portion of the curve. For each type of hydrogel, four samples were used for the compression test and the average value of four measurements for each sample was taken to represent the hydrogel mechanical property.

Temperature dependence of swelling ratios

For the study of temperature-dependent swelling, hydrogel samples were first equilibrated in a PBS solution at a temperature ranging from 23 (below LCST) to 80 °C (above LCST). The samples were allowed to swell in a PBS solution for at least 24 h at each predetermined temperature controlled up to ±0.1 °C by a thermostated water bath (Grant Precision Stirred Bath, Grant Instruments Ltd, Cambridge, England). After 24 h immersion in a PBS solution at a predetermined temperature, the hydrogel was removed from the water and blotted with a wet filter paper to remove excess water on the hydrogel surface and then weighted until a constant weight was reached. After this weight measurement, the hydrogel was re-equilibrated in a PBS solution at another predetermined temperature and its wet weight was determined thereafter. The dry weight of each sample was determined after drying to a constant weight under vacuum at 60 °C for overnight. The average values among three measurements were taken for each sample and the equilibrium swelling ratio (ESR) was calculated as follows,

$$\text{Swelling ratio} = W_s/W_d \quad (1)$$

where W_s is the weight of water in a swollen hydrogel at each temperature (wet weight – dry weight) and W_d is the dry weight of hydrogel.

Deswelling or shrinking kinetics

The shrinking kinetics of the hydrogels were measured gravimetrically at 60 °C. This temperature was chosen because it is well above LCST of PNIPAAm and would show more significant temperature-induced deswelling kinetics within a shorter time frame. The hydrogel samples were first immersed in a PBS solution at room temperature till it reached equilibrium (about 24 h). The equilibrated hydrogel samples were then quickly transferred into a water bath of 60 °C. At each pre-determined time, the samples were removed from the hot water and weighted after wiping off the excess water on surface with a wet filter paper. Water retention was defined as follows:

$$\text{Water retention} = [(W_t - W_d)/W_s] \times 100 \quad (2)$$

where W_t was the weight of the wet hydrogel at time t and 60 °C, W_s was the weight of water in swollen hydrogel at time 0 at room temperature and W_d was the dry weight of hydrogel.

Swelling kinetics

The freeze-dried hydrogel samples were immersed in a PBS solution at 22 °C and removed from water bath at regular time intervals. After wiping off the water on the surfaces of the samples with wet filter papers, the weights of hydrogels were recorded and the water uptake is defined as follows,

$$\text{Water uptake} = 100 \times [(W_t - W_d)/W_s] \quad (3)$$

where W_t is the weight of the wet hydrogel at time t and 22 °C and the other terms are the same as defined in Eq. (1) above.

Results and discussion

LCST behavior

During the phase separation in the P(NIPAAm-co-AMPSA) hydrogels upon heating, the transition temperature of such a phase separation would be detected. Here, the LCST of the P(NIPAAm-co-AMPSA) hydrogels was defined as the onset temperature of the endotherms [27]. Table 2 shows the LCSTs of P(NIPAAm-co-AMPSA) hydrogels. It was found that P(NIPAAm-co-AMPSA) hydrogels had higher LCSTs than a pure PNIPAAm hydrogel. A difference as high as 13.7 °C (or 43% higher) was found between Gel_0 (31.8 °C) and Gel_{10} (45.5 °C), owing to the presence of the AMPSA moiety, which provided a hydrophilic contribution to PNIPAAm.

The LCST data also show that an increase in the content of AMPSA in P(NIPAAm-co-AMPSA) hydrogel led to an incresing LCST of the copolymer hydrogels. For example, the LCST of $Gel_{2.5}$ was around 33.9 °C, while the LCST of Gel_5 and Gel_{10} were around 36.8 °C and 45.5 °C, respectively. When the AMPSA content reached 15 wt%, no LCST of the hydrogel (Gel_{15}) was detected. Thus, the introduction of AMPSA segment into PNIPAAm hydrogels affected the LCST of PNIPAAm. A similar effect on LCST was also found in our previous study, in which the incorporated hydrophilic Dex-MA segment into PNIPAAm increased the LCST of resulting Dex-MA/PNIPAAm hydrogels, but the effect was significantly smaller (about 12% increase) upon ¼ feed ratio of Dex-MA/NIPAAmn than our current AMPSA/NIPAAm system at 1/9 feed ratio (Gel_{10} with 43% increase at 1/9 ratio) [28]. The larger LCST increase in the AMPSA/NIPAAm system than the Dex-MA/NIPAAm system may be attributed to a much higher level ionization of the sulfonic group in AMPSA than the carboxylic acid group in Dex-MA that could result in more and stronger hydrogen bonds in the AMPSA/NIPAAm system, i.e., require higher temperature to break hydrogen bonds and hence higher LCST as observed.

Table 2 LCSTs of P(NIPAAm-co-AMPSA) hydrogels from DSC investigations

Hydrogel	Gel_0	$Gel_{2.5}$	Gel_5	Gel_{10}	Gel_{15}
Content (wt.%)[a]	0	2.5	5	10	15
LCST (°C)	31.8	33.9	36.8	45.5	/ [b]

[a] Weight percentage of AMPSA based on the amount of all monomers in the feed composition

[b] No LCST was found

Interior morphology

The interior morphology of swollen and freeze-dried hydrogels is shown in Fig. 1. The SEM data clearly illustrate the influence of the AMPSA on PNIPAAm-based hydrogel morphology. First, the introduction of AMPSA into PNIPAAm has dramatically changed the porous matrix from a round and shallow pores in a conventional PNIPAAm hydrogel to a well-defined honey-comb-like porous structure with rigid matrix wall in P(NIPAAm-co-AMPSA) hydrogels. In addition, the pore size of these honey-comb-like 3D structures increased with an increase in AMPSA content in the P(NIPAAm-co-AMPSA) hydrogel and reached the largest size in Gel_{15}, while Gel_0 had the smallest pore size. Conversely, Gel_0 showed the largest number of pores per unit area while the Gel_{15} had the smallest number of pores.

The enlarged porous network from $Gel_{2.5}$ to Gel_{15} was attributed to the ionic hydrophilic property of the incorporated AMPSA moiety. When a pure PNIPAAm hydrogel swells in water at room temperature (<LCST), there exist hydrogen bond interactions between amide groups of PNIPAAm chains and surrounding water. These interactions may lead to the formation of cage-like structures around hydrophobic groups, i.e. structured water molecules surround the hydrophobic groups, which results in swelling of PNIPAAm hydrogels in water [29, 30]. With the introduction of AMPSA, P(NIPAAm-co-AMPSA) hydrogels might exhibit special network structure due to the formation of two types of hydrogen bond that pure PNIPAAm doesn't have: hydrogen bond between SO_3^- and water and hydrogen bond between amide and $-SO_3^-$ groups. As a result, there is a competition for water in the P(NIPAAm-co-AMPSA) hydrogels. In a pure PNIPAAm hydrogel, water was attracted toward amide groups in PNIPAAm chains and the attracted water molecules acted cooperatively to form an iceberg-like structure of water at the molecular level as mentioned above. With the introduction of AMPSA in P(NIPAAm-co-AMPSA) hydrogels, due to a much higher ionization and stronger hydrophilic characteristic of

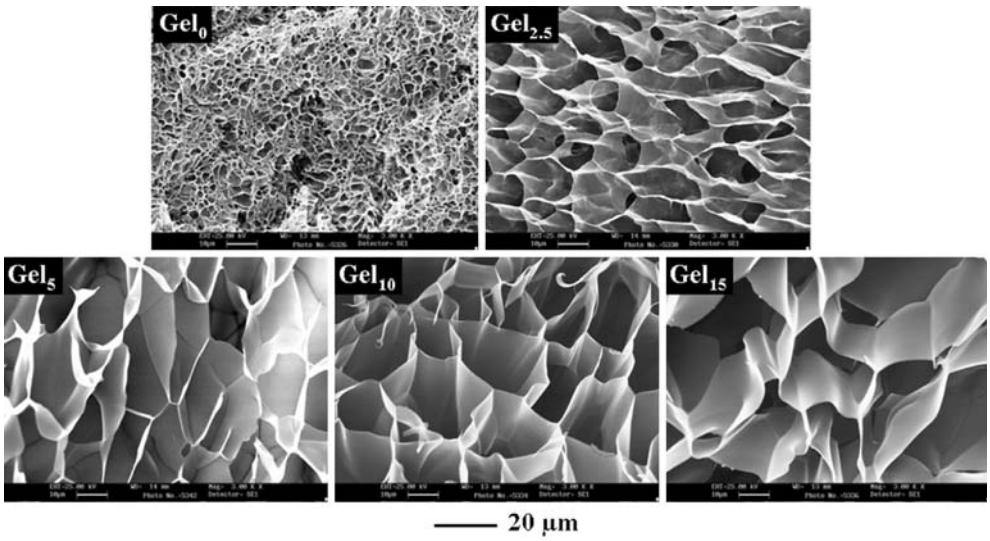

Fig. 1 Effect of precursors' feed ratio on the interior morphologies of swollen P(NIPAAm-co-AMPSA) hydrogels (before the SEM observations, freeze-dried samples were fractured carefully to exhibit their interior morphologies.). Refer to Table 1 for the composition of Gel label

the $-SO_3^-$ group in AMPSA segments, this $-SO_3^-$ group could attract more water than the amide group in PNIPAAm segments; and the water attracted to the AMPSA segments might assemble into a better and more organized structure than those waters attracted to the amide group of PNIPAAm segments. Thus, more water could be attracted and contained in P(NIPAAm-co-AMPSA) than pure PINIPAAm hydrogels, i.e., the swelling capacity of P(NIPAAm-co-AMPSA) hydrogels was much improved when comparing to pure PNIPAAm hydrogels. Besides the effect of stronger hydrogen bonds, there existed strong electrostatic repulsions between highly ionized $-SO_3^-$ groups in P(NIPAAm-co-AMPSA) hydrogels. This repulsion would also facilitate the expansion of the hydrogel network, i.e., enlarged pores for a higher water uptake.

The presence of $-SO_3^-$ group in P(NIPAAm-co-AMPSA) hydrogels could also provide much stronger intermolecular hydrogen bonds between hydrophilic amide groups in PNIPAAm segments and $-SO_3^-$ groups in AMPSA segments due to the highly ionized nature of the $-SO_3^-$ groups. These strong intermolecular hydrogen bonds between amide groups and $-SO_3^-$ groups facilitate the macromolecules to assemble into a better and more organized matrix structure, which may provide certain structural stability and thus lead to the formation of well-defined honey-comb-like porous structure with rigid cell wall as observed in Fig. 1.

The distinctive 3D honey–comb porous structure upon swelling is also found in our previous study of PNIPAAm/Dextran-maleic acid hybrid hydrogel system [28, 31]. In those studies, upon swelling, distinctive ordered honey-comb-like porous network structure was observed as hydrophilic dextran-maleic acid (Dex-MA) segments were incorporated into PNIPAAm via crosslinking. However, an increasing hydrophilic Dex-MA content in a Dex-MA/PNIPAAm hydrogel system led to a reduction in pore size rather than the finding in the current study that an increase in hydrophilic AMPSA content led to an increase in pore size of AMPSA/PNIPAAm hydrogels. This observed difference between the PNIPAAm/Dex-MA system and our current P(NIPAAm-co-AMPSA) system is mainly due to the difference in crosslinking level. In a PNIPAAm/Dex-MA hydrogel system, Dex-MA was used as the crosslinker as well as the co-precursor since the crosslinkable groups in Dex–MA are located along the anhydroglucose units of dextran backbone chains. In the P(NIPAAm-co-AMPSA) system, hydrophilic AMPSA was solely used as the co-monomer (*N*, *N*′-methylenebisacrylamide as a crosslinker), and hence an increase in AMPSA content would not increase the crosslinking level as Dex-MA did in the Dex-MA/PNIPAAm hydrogels.

Mechanical property

The mechanical property of swollen P(NIPAAm-co-AMPSA) hydrogels (measured in terms of initial compression modulus) as a function of the feed ratio of AMPSA to NIPAAm is shown in Fig. 2. The data exhibit that the compression moduli of the P(NIPAAm-co-AMPSA) hydrogels were reduced from a pure PNIPAAm hydrogel (Gel_0, 5.4 KPa) when AMPSA was first incorporated into PNIPAAm at a 5/195 feed ratio ($Gel_{2.5}$, 4.1KPa). However, a further increase in AMPSA/NIPAAm feed ratio led to a significant increase in the compression modulus of P(NIPAAm-co-AMPSA) hydrogels to about 9 KPa (Gel_5 = 8.8 KPa, Gel_{10} = 9.0 KPa and Gel_{15} = 9.2 KPa).

The change in mechanical property with AMPSA/NIPAAm feed ratio could be attributed to the resulting morphological structure of the (NIPAAm-co-AMPSA) hydrogels shown in Fig. 1. The initial reduction in

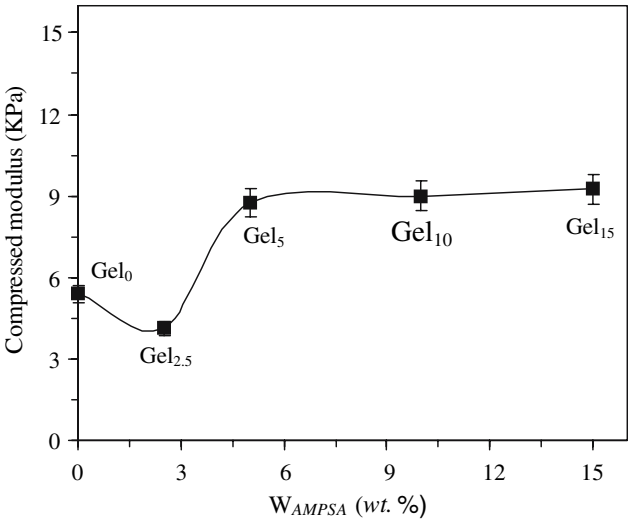

Fig. 2 Effect of precursors' feed ratio on the initial compression modulus of the swollen P(NIPAAm-co-AMPSA) hydrogels

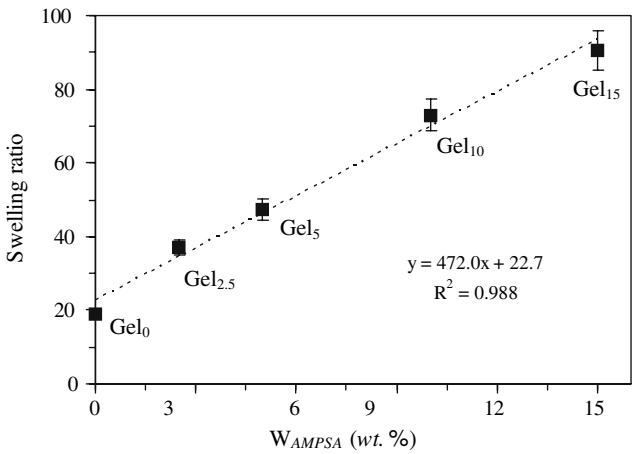

Fig. 3 Effect of precursors' feed ratio on the equilibrium selling ratios of P(NIPAAm-co-AMPSA) hydrogels at room temperature

compression modulus of $Gel_{2.5}$ is attributed to the enlarged porous structure when comparing to Gel_0. Generally, a macroporous network would have a lower mechanical property because polymer mass per unit volume is reduced. The higher compressive moduli of Gel_5, Gel_{10} and Gel_{15} were probably attributed to the very regular and relatively more rigid cell wall structure. A similar effect of polyelectrolytes on the improvement of mechanical property of hydrogels was also reported by Philippova et al. [32]. In their study of polyacrylamide hydrogel with embedded synthetic polyelectrolyte, poly(4,4″-(disodium 2,5-dimethyl-1,1′:4′,1″-terphenyl-3′,2″-disulfonate), it was shown that the incorporation of the polyelectrolyte within the uncharged polyacrylamide network improved the mechanical strength of the hydrogel because electrostatic attractions between polyelectrolytes and polyacrylamide hydrogels made the hydrogel macromolecules more rigid, and this presence of stiff elements in the hydrogel resulted in higher mechanical property.

Equilibrium swelling ratios (ESR) at room temperature

Figure 3 shows the effect of AMPSA/NIPAAm feed ratio on equilibrium swelling ratios (ESR) of P(NIPAAm-co-AMPSA) hydrogels at room temperature. The data show that the swelling ratio of hydrogels at room temperature (below their LCST) increased linearly with the AMPSA contents (from Gel_0 to Gel_{15}). For example, ESR of $Gel_{2.5}$ (37) and Gel_{15} (91) are about double and five times of the one of Gel_0 (19), respectively.

This increase in ESR with AMPSA contents in P(NIPAAm-co-AMPSA) hydrogels was attributed to the hydrophilic nature of AMPSA in hydrogel network. It is known that a hydrophilic/hydrophobic balance exists in the PNIPAAM network because of its hydrophilic and hydrophobic segments. As additional hydrophilic AMPSA segments were introduced into the backbone of the PNIPAAm hydrogel, the hydrophilic/hydrophobic balance of the resulting hydrogel network was shifted toward more hydrophilic, leading to an increasing in water content at room temperature, i.e., higher swelling ratio than pure PNIPAAm hydrogel. In addition, the increasing swelling ratio from Gel_0 to Gel_{15} at room temperature is consistent with their morphology observed (see Fig. 1). As described above, an increase in the content of AMPSA moiety from Gel_0 to Gel_{15} led to a more open and larger porous network structure of the corresponding hydrogel, that is, an improved swollen capacity or water uptake due to an increasing void volume for accommodating more water.

The increasing swelling ratio at room temperature with increasing AMPSA content in P(NIPAAm-co-AMPSA) hydrogels is contrary to our prior findings in PNIPAAm/Dex-MA hydrogels [28], where the swelling ratio of PNIPAAm/Dex-MA hydrogels decreased with an increase in hydrophilic Dex–MA content. Such a difference in hydrophilic moiety dependent swell ratio could be attributed to different crosslinking level. In PNIPAAm/Dex-MA hydrogels, the hydrophilic Dex–MA moiety also acted as a crosslinking agent as previously discussed (interior morphology and mechanical property). Hence an increase in Dex–MA content in Dex–MA/PNIPAAm hydrogels increased the crosslinking density of the resulting hydrogels, which could greatly limited the expansion of hydrogel network, i.e., reduced swelling ratio at room temperature. In the current study of PNIPAAm/AMPSA system, hydrolytic AMPSA moiety was used as a co-monomer solely, its hydrophilic property would improve the hydrophilicity of the resulting P(NIPAAm-co-AMPSA) hydrogels, leading to increasing swelling ratios with increasing AMPSA content.

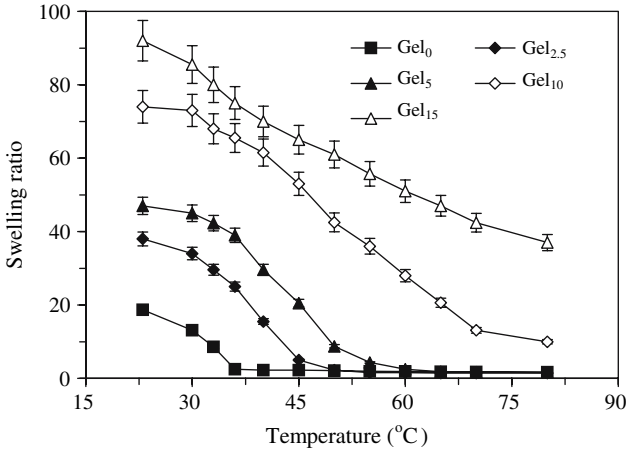

Fig. 4 Effect of precursors' feed ratio on the temperature dependence of equilibrium swelling ratios of P(NIPAAm-co-AMPSA) hydrogels over the temperature range from 23 to 80 °C

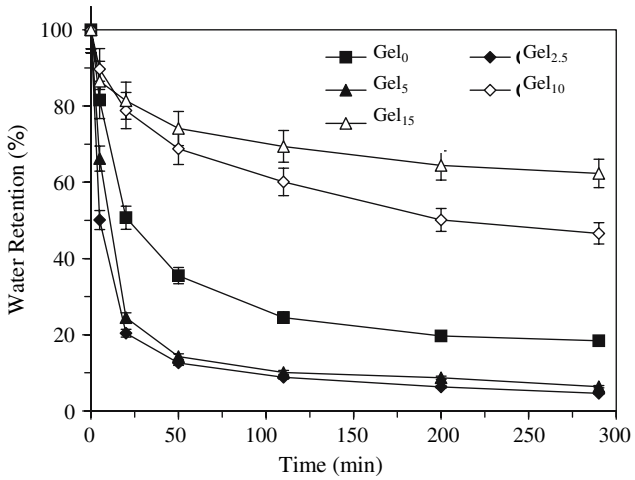

Fig. 5 Effect of precursors' feed ratio on the shrinking kinetics of P(NIPAAm-co-AMPSA) hydrogels in PBS solution at 60 °C

Temperature dependence in swelling ratios

Figure 4 demonstrates the classical temperature dependence of swelling ratios (SR) of P(NIPAAm-co-AMPSA) hydrogels over a temperature range from 23 (<LCST) to 80 °C (>LCST). The data show that all the hydrogels exhibited a temperature-induced reduction in swelling ratio, a classical characteristic of PNIPAAm-based material; but the incorporation of the AMPSA moiety into PNIPAAm backbone improved the magnitudes of the thermo-induced shrinkage. For example, as temperature changed from 23 to 70 °C, the swelling ratio of a pure PNIPAAm hydrogel (Gel_0) reduced from 18.7 to 1.7, with a Δ swelling ratio of 17 (= $SR_{23\ °C}$–$SR_{70\ °C}$). Over the same temperature range, Δ swelling ratios of $Gel_{2.5}$, Gel_5, and Gel_{10} were 37, 45, and 61, respectively. The Δ swelling ratio, however, decreased to 50 in Gel_{15}.

The increasing magnitude of Δ swelling ratio observed in P(NIPAAm-co-AMPSA) hydrogels appears to be attributed to the macroporous structure and initially larger amounts of water content at 23 °C. As a result, when immersed in hot water at 70 °C, more water could be extruded, i.e., higher magnitude of Δ swelling ratio. As to Gel_{15}, its reduced magnitude of Δ swelling ratio from Gel_{10} could be due to a weakened thermo-responsive capability from higher amounts of thermo-nonresponsive AMPSA moiety which could dilute the thermo-responsive capability of PNIPAAm. As a result, the shrinkage of Gel_{15} was not complete and certain amounts of water still remained in the large porous Gel_{15} network at 70 °C.

Shrinking kinetics

The shrinking kinetics of P(NIPAAm-co-AMPSA) hydrogels upon temperature change from 22–60 °C were shown in Fig. 5. The shrinking data show that the shrinking rate of P(NIPAAm-co-AMPSA) hydrogels were faster than pure PNIPAAm hydrogel (Gel_0) when the AMPSA content was not high (i.e., $Gel_{2.5}$ and Gel_5). For instance, $Gel_{2.5}$ or Gel_5 had their water retentions reduced from 100% to nearly 13–14% within 50 min, and 5–6% within 290 min respectively. During the same time interval, Gel_0, however, showed deswelling to only 36% (50 min) and 18% (290 min). This advantage of faster deswelling rate at $Gel_{2.5}$ and Gel_5 disappeared as the AMPSA contents increased further (i.e., Gel_{10} or Gel_{15}), and their deswelling rates were slower than the pure PNIPAAm control.

The improved shrinking rate of $Gel_{2.5}$ or Gel_5 was attributed to the macroporous structure of P(NIPAAm-co-AMPSA) hydrogels as seen in Fig. 1. It is well known that in a PNIPAAm system, macroporous network structure exhibits faster temperature-induced response rate because freed water could diffuse out quickly and timely [33–35]. In the P(NIPAAm-co-AMPSA) hydrogels, their macroporous structure appeared to have larger pores than pure PNIPAAm (Fig. 1) which led to higher initial swelling ratio at 22 °C. When external temperature was altered from 22 to 60 °C, hydrogen bonds were broken, and more water in P(NIPAAm-co-AMPSA) hydrogels were freed quickly due to the hydrophobic interactions between isopropylamide pendant groups. Consequently, more freed water was extruded, that is, P(NIPAAm-co-AMPSA) hydrogels exhibited faster shrinking rate at 60 °C than pure PNIPAAm.

A comparison between our previous findings in PNIPAAm/Dex-MA system [28] and the results in this research (PNIPAAm/AMPSA system) suggests that incorporating either Dex-MA or AMPSA ionic moiety into PNIPAAm system might result in a similar effect on response rate of the PNIPAAm-based copolymers, i.e. faster shrinking

dynamics. However, there are also some differences between these two systems. One of the main differences is the different ionization degree of ionizable groups between Dex-MA and current AMPSA moieties. As we know, maleic acid in PNIPAAm/Dex-MA system is a weak acid, while the sulfonic acid in the current PNIPAAm/AMPSA system is a strong acid. Because of this difference in acidity strength between maleic acid and sulfonic acid, the ionization degree of maleic acid is much sensitive to pH changes of the swelling medium than sulfonic acid. For example, PNIPAAm/Dex-MA hydrogels were reported to have a high pH sensitivity in the pH range from 3 to 7 [28, 31]. In the case of P(NIPAAm-co-AMPSA) hydrogels, our unpublished preliminary testing of the effect of pH (3.0–10.0) on the swelling capability at room temperature indicated that there was no obvious difference in equilibrium swelling ratio within the pH range studied.

The deswelling rate of PNIPAAm-based hydrogels also depends on the nature of the skin layer formed upon the collapse of network structure. Figure 6 shows the SEM images of the surface of two P(NIPAAm-co-AMPSA) hydrogels and a pure PNIPAAm control collapsed at 60 °C. Gel_0 and Gel_5 showed dense and smooth surface with few pores; Gel_{15} , however, showed a far more open porous surface structure, an indication of less complete structural collapse at 60 °C. Such a less complete collapse at 60 °C would provide additional void volume for accommodating water, i.e., a slower shrinking rate of Gel_{15} at 60 °C. Beside this morphological reason, the slower deswelling rate of the P(NIPAAm-co-AMPSA) hydrogels having higher AMPSA contents (Gel_{10} and Gel_{15}) could also attributed to the more dilution of the thermo-responsive capability of PNIPAAm at such high AMPSA contents. Such a dilution would also reduce the thermo-responsive rate.

Swelling kinetics

The swelling kinetics of P(NIPAAm-co-AMPSA) hydrogels at 22 °C were shown in Fig. 7. It is clear that an increasing AMPSA content in P(NIPAAm-co-AMPSA) hydrogels resulted in a higher swelling or hydration rate at 22 °C. This relationship suggests that water can diffuse into P(NIPAAm-co-AMPSA) hydrogel networks faster if the hydrogel had more AMPSA contents. In the case of a pure PNIPAAm hydrogel (Gel_0), it absorbed about 8% water within first 5 min, and about 47% at the end of 140 min. However, $Gel_{2.5}$ and Gel_{15} absorbed about 26 and 56% water within 5 min, and about 82 and 97% within 140 min, respectively. The improved swelling rate was attributed to the hydrophilic and highly ionized nature of incorporated AMPSA moiety in P(NIPAAm-co-AMPSA) hydrogels. In addition, the larger porous network of P(NIPAAm-co-AMPSA) hydrogels is also a crucial factor to accelerate the swelling rate during the hydration process at 22 °C.

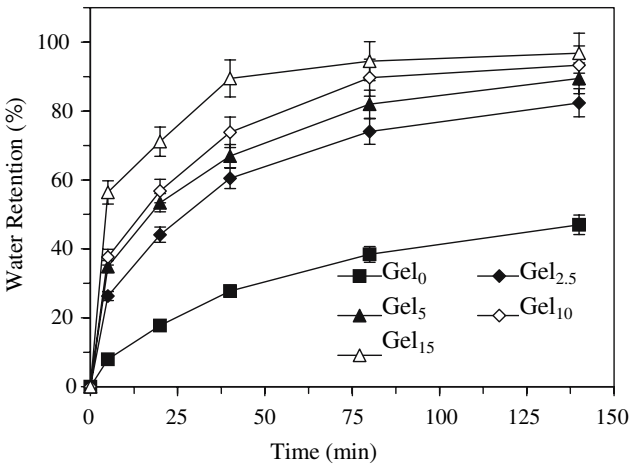

Fig. 7 Effect of precursors' feed ratio on the swelling kinetics of P(NIPAAm-co-AMPSA) hydrogels in PBS solution at 22 °C

Conclusions

A new family of P(NIPAAm-co-AMPSA) hydrogels was synthesized and characterized. The influence of polyelectrolyte moiety (AMPSA) on the thermosensitive property of PNIPAAm hydrogels was investigated. The incorporation of AMPSA co-monomer into PNIPAAm backbone resulted in a honey-comb-like porous network structure with rigid cell wall structure. The mechanical property of P(NIPAAm-co-AMPSA) hydrogels was strengthened due

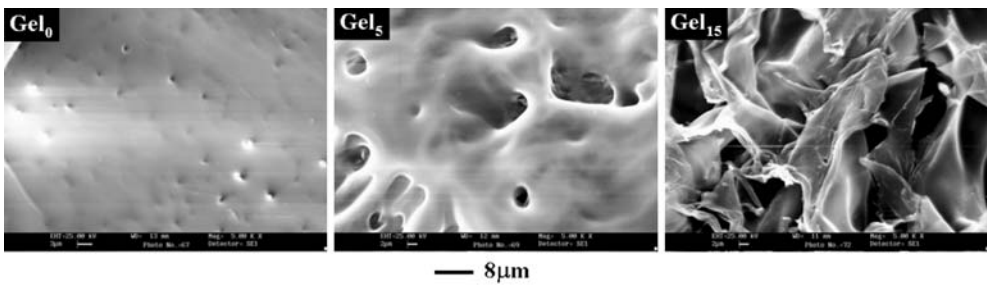

Fig. 6 Surface morphologies of P(NIPAAm-co-AMPSA) hydrogels after shrinking in hot water (60 °C) for 24 h

to the rigid cell wall as well as well-organized ordered porous structure. Because of the hydrophilic and strong ionic nature of the AMPSA segment, the LCST, swelling capability at room temperature and shrinking rate upon heating of P(NIPAAm-co-AMPSA) hydrogels were also significantly altered.

References

1. K. N. PARK, W. S. W. SHALABY and H. S. PARK, 1975 *Biodegradable hydrogels for drug delivery* (Technomic Publication AG. Lancaster, PA) pp. 1–9, chapter 1
2. N. A. PEPPAS and A. G. MIKOS, Preparation methods and structure of hydrogels. *Hydrogels in Medicine and Pharmacy,* edited by N.A. Peppas, Vol.1. CRC Press, Boca Raton, FL, 1986, 1–27
3. A. SILBERBERG, Network deformation in Flow. *Molecular basis of polymer. Networks*, edited by A. Baumgartner and C.E. Picot, Berlin: Spring-Verlag, 1989, 147–151
4. B. D. RATNER and A. S. HOFFMAN, Synthetic hydrogels for biomedical applications. *Hydrogels for Medical and Related Applications,* edited by J.D. Andradre, ACS Symposium Series, American Chemical Society, Washington. D.C., 1976, 31, 1–36
5. G. CHEN and A. S. HOFFMAN, *Nature* **373** (1995) 49
6. A. M. MIKA, R. F. CHILDS, J. M. DICKSON, B. E. MCCARRY and D. R. GAGNON, *J. Membr. Sci.* **108** (1995) 37
7. Y. HIROSE, G. GIANNETTI, J. MARGUARDT and T. TANAKA, *J. Phys. Soc. Jpn.* **61** (1992) 4085
8. J. P. GANG, J. KAWAKAMI, V. G. SERGEYEV and Y. OSADA, *Macromolecules* **24** (1991) 5246
9. T. MIYATA, N. ASAMI and T. URAGAMI, *Nature* **399** (1999) 766
10. Y. HIROKAWA and T. TANAKA, *J. Chem. Phys.* **81** (1984) 6379
11. H. FEIL, Y. H. BAE, J. FEIJEN and S. W. KIM, *Macromolecules* **26** (1993) 2496
12. H.G. SCHILD, *Prog. Polym. Sci.* **17** (1992) 163
13. Y. H. BAE, T. OKANO and S. W. KIM, *J. Polym. Sci. Part B Polym. Phys.* **28** (1990) 923
14. N. A. PEPPAS and R. LANGER, *Science* **263** (1994) 1715
15. P. S. STAYTON, T. SHIMOBJI, C. LONG, A. CHILKOTI, G. CHEN, J. M. HARRIS and A. S. HOFFMAN, *Nature* **378** (1995) 472
16. J. KOST and R. LANGER, *Adv. Drug Deliver. Rev.* **6** (2001) 125
17. T. SHIROYA, N. TAMURA, M. YASUI and K. FUJIMOTO, *Colloid Surf. B* **4** (1995) 267
18. I. Y. GALAVE, M. N. GUPTA and B. MATTIASSON, *Chemtech.* **26** (1996) 19
19. H. FEIL, Y. H. BAE, J. FEIGEN and S. W. KIM, *J. Membr. Sci.* **64** (1991) 283
20. F. ROSSO, A. BARBARISI, M. BARBARISI, O. PETILLO, S. MARGARUCCI, A. CALARCO and G. PELUSO, *Mater. Sci. Engi. C* **23** (2003) 371
21. J. K. ANDRADE, S. NAGAOKA, S. COOPER, T. OKANO and S. W. KIM, *Trans. – Am. Soc. Artif. Intern. Organs* **83** (1987) 75
22. B. D. RATNER, A. B. JOHNSTON and T. J. LENK, *J. Biomed. Mater. Res. Appl. Biomater.* **21** (1987) 59
23. S. W. Kim and J. Feijens, *CRC Critical Reviews in Biocompatibility,* edited by D. Williams, Vol. 1(3). CRC Press, Boca Raton, FL. 1985, 229–241
24. Y. OSADA, H. OKUZAKI and H. HORI, *Nature* **355** (1992) 242
25. H. OKUZAKI and Y. OSADA, *Electrochim. Acta.* **40** (1995) 2229
26. Y. UEOKA, J. P. GONG and Y. OSADA, *J. Intelligent Mat. Syst. Str.* **8** (1997) 465
27. X. Z. ZHANG, D. Q. WU and C. C. CHU, *Biomaterials* **25** (2004) 3793
28. X. Z. ZHANG, D. Q. WU and C. C. CHU, *Biomaterials* **25** (2004) 4719
29. H. TANAKA, H. TOUHARA, K. NAKANISHI, N. WATANABE, *J. Chem. Phys.* **80** (1984) 5170
30. K. OTAKE, H. INOMATA, M. KONNO, S. SAITO, *Macromolecules* **23** (1990) 283
31. S. NAMKUNG, C. C. CHU, *J. Biomater. Sci.* (In Press)
32. O. E. PHILIPPOVA, R. RULKENS, B. I. KOVTUNENKO, S. S. ABRAMCHUK, A. R. KHOKHLOV and G. WEGNER, *Macromolecules* **31** (1998) 1168
33. X. S. WU, A. S. HOFFMAN and P. YAGER, *J. Polym. Sci., Part A Polym. Chem.* **30** (1992) 2121
34. X. Z. ZHANG, Y. Y. YANG, T. S. CHUNG and K. X. MA, *Langmuir* **17** (2001) 6094
35. R. X. ZHUO and W. LI, *J. Polym. Sci. A Polym. Chem.* **41** (2003) 152